




Direct versus indirect excitation of ultrafast magnetization dynamics in FeNi alloys

Clemens von Korff Schmising ^{1,*}, Somnath Jana ¹, Ole Zülich,¹ Denny Sommer,¹ and Stefan Eisebitt ^{1,2}

¹Max-Born-Institut für Nichtlineare Optik und Kurzzeitspektroskopie, Max-Born-Straße 2A, 12489 Berlin, Germany

²Technische Universität Berlin, Institut für Optik und Atomare Physik, 10623 Berlin, Germany



(Received 21 November 2023; accepted 9 February 2024; published 12 March 2024)

Ultrafast demagnetization can be induced either coherently by direct interaction with the optical light field or indirectly via excitation of the electron system, which subsequently couples to the magnetization. An intriguing direct process is optical intersite spin transfer (OISTR), which changes the local magnetic moments during the optical absorption process itself and leads to a potentially coherent net spin transport between two magnetic subsystems. In this paper, we find that both direct and indirect excitation of an FeNi alloy result in identical experimental signatures in transverse magneto-optical measurements in the extreme ultraviolet spectral range, which has been previously interpreted as evidence for the OISTR effect: a delayed onset of the ultrafast response of Ni with respect to Fe as well as an increasing signal for photons probing energies below the Ni resonance. Our findings align with recent theoretical and experimental investigations, which propose alternative explanations of these experimental observations and do not rely on a direct and coherent interaction between light and spin. Instead, the distinctly different magnetization dynamics of Fe and Ni may be governed by intersite spin transfer driven by electron scattering or be the result of element-specific microscopic properties such as inhomogeneous spin-orbit coupling or electron magnon scattering.

DOI: [10.1103/PhysRevResearch.6.013270](https://doi.org/10.1103/PhysRevResearch.6.013270)

I. INTRODUCTION

Coherent optical control of magnetization relies on a direct interaction between the optical light field and the magnetic system. However, to date most microscopic mechanisms in femtomagnetism in metallic systems have been identified to be secondary processes driven by an excess of energy in the electronic system gained after optical excitation. Prominent examples are spin-orbit induced spin-flip scattering [1], equilibration of the chemical potentials [2,3], magnon generation [4–8], or spin transport [9]. Indeed, a series of experiments were able to demonstrate that indirect excitation via hot electrons suffices to induce efficient demagnetization [10,11] or even lead to deterministic, all-optical switching of the magnetization direction [12–15]: a femtosecond laser pulse excites an optically opaque metallic layer generating a hot electron distribution, which is then injected into an adjacent magnetic layer via ballistic or superdiffusive transport.

Only with the seminal work of Dewhurst *et al.* [16], the concept that the light field itself can directly manipulate the magnetization was revived: time-resolved density-of-state calculations predicted that in multicomponent magnetic systems optical excitation can efficiently redistribute spin-polarized carriers between the different sublattices, leading to a local

change of the magnetic moment within the temporal duration of the light pulse. The process is called optical intersite spin transfer (OISTR) and within a few years several experiments reported evidence for such direct spin manipulation by light [17–22]. The majority of these experiments employed ultrafast spectroscopy in the extreme ultraviolet (XUV) spectral range to follow the element-specific magnetization via resonant $3p$ -to- $3d$ transitions. Particularly well-suited model systems are alloys consisting of two elements with a distinctly different number of available states above the Fermi energy such that optical excitation leads to a preferential direction of a potential intersite spin transfer. In FeNi alloys, for example, one expects a preferential transfer of Ni minority carriers into available states of Fe, which would lead to a transient increase of the Ni moment and a concomitant accelerated decrease of the Fe moment.

Accordingly, Hofherr *et al.* [20] identified two experimental observations in XUV transverse magneto-optical Kerr (T-MOKE) measurements as evidence for such intersite spin transfer in an FeNi alloy.

(i) The delay in the evolution of the magnetic asymmetry, A , observed between the ultrafast response measured at the Ni $M_{2,3}$ edge with respect to Fe $M_{2,3}$ edge is interpreted as a competition between OISTR and secondary demagnetization processes.

(ii) The observation of an asymmetry increase for photons below the Ni resonance is understood as an indication for a magnetization increase for states below the Fermi energy, E_F , which have become available after laser excitation of Ni minority carriers.

Arguing along similar lines, an increase of the asymmetry detected at the Co $M_{2,3}$ edge in the half metallic Co_2MnGe

*korff@mbi-berlin.de

Published by the American Physical Society under the terms of the Creative Commons Attribution 4.0 International license. Further distribution of this work must maintain attribution to the author(s) and the published article's title, journal citation, and DOI.

Heusler alloy was interpreted as an intersite spin transfer during the optical absorption process [21].

However, recent theoretical work suggests that exchange scattering between two sublattices may also lead to efficient and ultrafast intersite spin transfer offering a theoretical explanation for the experimental observations without invoking direct and coherent interaction between the light and the magnetization [23]. A quantum theory of ultrafast spin dynamics, where intersite spin transfer among different sublattices in transition metal alloys is driven by intersite electron hopping, however, concluded that the governing time scales on the order of ≈ 1 fs are too short to rationalize the delayed demagnetization of Ni on the order of tens of femtoseconds. Instead, element-specific spin-orbit coupling strengths are shown to agree with the experimental observations of the distinct Fe and Ni magnetization response [24]. Similarly, a combination of theory and experiment showed that different magnon scattering efficiencies between the Fe and Ni sublattices can explain the delayed loss of Ni magnetization with respect to Fe after optical excitation [25,26].

In this research, we conduct an experiment to test the hypothesis that direct and coherent light-driven spin transfer is the primary microscopic process leading to the distinctly different ultrafast demagnetization dynamics of Fe and Ni. To achieve this objective, we systematically compare the ultrafast response of an $\text{Fe}_{50}\text{Ni}_{50}$ alloy after *direct*, optical excitation and after *indirect* excitation via hot electrons generated in an optically thick aluminium capping layer. We employ XUV T-MOKE spectroscopy probing the Fe and Ni $M_{2,3}$ edge and show that the two fingerprint observables, a delayed onset of the Ni demagnetization, as well as an asymmetry increase for photons tuned to energies below the Ni edge are found for *both* excitation geometries. These findings cast doubt on the significance of prior experimental evidence for the OISTR effect.

II. EXPERIMENT

Two samples with the composition glass/Ta(2 nm)/ $\text{Fe}_{0.5}\text{Ni}_{0.5}$ (5 nm)/Al(30 nm), in the following referred to as FeNi/Al(30 nm), and glass/Ta(3 nm)/ $\text{Fe}_{0.5}\text{Ni}_{0.5}$ (5 nm)/Al(3 nm), in the following referred to as FeNi/Al(3 nm), are deposited via electron beam evaporation. Both samples exhibit an in-plane magnetization with a square hysteresis loop characterized by a low coercive field of below 10 mT. Additionally, we evaporated a single aluminium layer with a thickness of 30 nm on an identical glass substrate for an accurate characterization of its optical properties.

We employ a T-MOKE geometry in the XUV spectral range between 47 and 72 eV to probe the element-specific ultrafast magnetization dynamics of the FeNi alloy as schematically shown in Fig. 1. The XUV radiation is produced via high harmonic generation (HHG) focusing laser pulses from a Ti:sapphire based amplifier system with a pulse duration of 25 fs, a repetition rate of 3 kHz, a pulse energy of ≈ 2.5 mJ, and a wavelength range of $\lambda = (800 \pm 50)$ nm into a gas cell filled with helium. The resulting XUV spectrum is characterized by narrow bandwidth emission peaks, spaced by ≈ 3.1 eV covering the broad resonances of the Fe and Ni $M_{2,3}$ edges around 54 and 66 eV, respectively. The

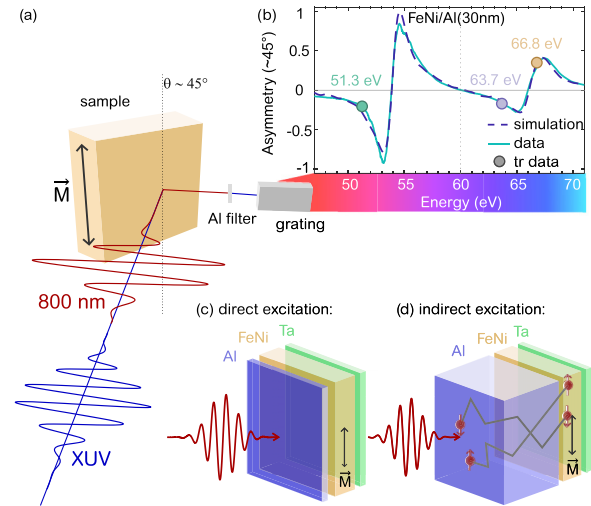


FIG. 1. (a) Illustration depicting the configuration of the T-MOKE setup using optical pump light at $\lambda = 800$ nm and probe light in the XUV spectral range between 47 and 71 eV. (b) Measured (solid line) and calculated (dotted line) magnetic asymmetry data as a function of XUV probe photon energies. Time-resolved measurements were performed at photon energies resonant with either the Fe $M_{2,3}$ edge (51.3 eV) or Ni $M_{2,3}$ edge (63.7 and 66.8 eV) and are marked by round dots. Panels (c) and (d) illustrate the configuration for direct and indirect excitation of the FeNi/Al(30 nm) and FeNi/Al(30 nm) samples, respectively.

p -polarized XUV light pulses are reflected off the sample and detected by a spectrometer. An electromagnet toggles the magnetization direction, \vec{M} , of the sample between the two directions perpendicular to the plane of incidence. The T-MOKE observable, defined as the normalized difference of the reflectance for opposite magnetization directions, is called the magnetic asymmetry, A . Choosing an incidence angle of $\theta \approx 45^\circ$ in the vicinity of the Brewster angle maximizes A . In order to confirm a direct proportionality between observable A and magnetization, we compute the wave propagation within the nanostructure, considering reflection and refraction at interfaces as outlined in Schick [27] and using atomic and magnetic form factors from literature sources [19,28]. A comparison between the calculated and measured asymmetry is shown in Fig. 1(b). The dotted vertical line at 60 eV separates the spectral regions where A is either dominated by Fe or Ni, determined by setting the respective magnetic moment to zero in the simulation [29]. While the asymmetry at the photon energies of 51.3 eV (Fe $M_{2,3}$) as well as 63.7 eV (below Ni $M_{2,3}$) and 66.8 eV (Ni $M_{2,3}$) scales linearly with the magnetic moments, we find strong nonlinearities at the maxima of the Fe asymmetry between 52.02 and 53.7 eV [30]. The ultrafast magnetization dynamics is triggered by laser pulses with a center wavelength of $\lambda = 800$ nm and a pulse duration of 30 fs at the sample position. The experiment's temporal resolution is determined by evaluating the cross correlation between optical pump and XUV probe pulses, yielding a value of 35 fs. A more detailed description of the experimental layout can be found in a dedicated paper on our instrument [31].

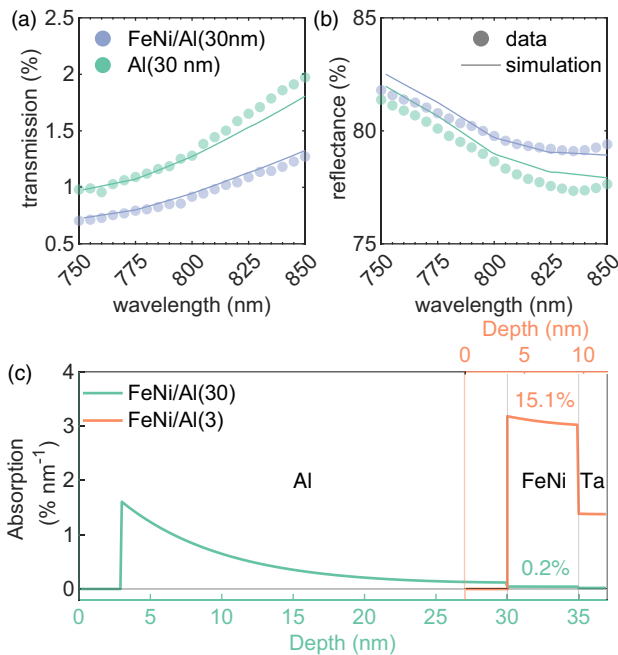


FIG. 2. Measured and calculated (a) transmission and (b) reflectance of p -polarized light centered at a wavelength of $\lambda = 800$ nm for the reference Al(30 nm) and the FeNi/Al(30 nm) sample. Panel (c) shows the absorption depth profile for both investigated samples FeNi/Al(3 nm) and FeNi/Al(30 nm). The total absorption within the magnetic alloy FeNi amounts to 15.1 and 0.2%, respectively.

III. RESULTS

A. Optical absorption of Al

Aluminum combines three key physical properties to implement an indirect excitation geometry in T-MOKE experiments in the XUV spectral range.

(i) It exhibits a long mean free path of laser-excited electrons, leading to a predominately ballistic electron transport [32,33] and therefore to an efficient and ultrafast indirect excitation of the FeNi layer.

(ii) The absorption cross section of Al in the XUV spectral range is very small [28], allowing one to efficiently probe the buried FeNi layer.

(iii) For our excitation wavelength in the infrared spectral range the absorption is very strong, ensuring negligible direct interaction with the magnetic layer.

The latter point we have examined in more detail, by combining measurements and calculations to determine the optical properties of the Al capping layers for p -polarized radiation at an incidence angle of 45° in the wavelength range from 750 to 850 nm. The results are shown in Fig. 2 for (a) transmission and (b) reflectance and are compared to calculations based on a matrix transfer formalism [34] with tabulated indices of refraction [35]. We assume an oxidized aluminium top layer with a thickness of 3 nm [36], but otherwise use no further free parameters in the simulation. The quantitative agreement suggests that the absorption of the evaporated aluminium layer can be well described using the literature values. We demonstrate its optical opaqueness required for an indirect excitation

scheme by calculating the depth dependent absorption profile for both samples FeNi/Al(3 nm) and FeNi/Al(30 nm) [37]. The results are summarized in Fig. 2(c), where we show that the total absorption within the FeNi layer decreases from 15.1 to 0.2% when capping the system with an Al(30 nm) layer. We note that due to the 45° incidence angle the effective aluminium thickness amounts to ≈ 40 nm, in very close correspondence to the Al layer thickness used in Vodungbo *et al.* [10]. In our case, the aluminium layer reduces the relative direct interaction between the optical radiation and the magnetic alloy by a factor of approximately 76.

B. Ultrafast dynamics

The central experimental results of this paper are shown in Figs. 3(a) and 3(b), where we compare the ultrafast response of the FeNi alloy after direct and indirect excitation. The incident fluences were set to $f_{\text{dir}} = 3.5$ mJ/cm² and $f_{\text{ind}} = 39$ mJ/cm², respectively. Taking into account the different absorption profiles, this leads to an approximately seven times smaller optical absorption within the FeNi alloy for the indirect excitation. For both types of excitation, the magnetic asymmetry exhibits an ultrafast decrease, reaches a minimum of $A(t \approx 500$ fs) = 0.8, and then recovers on a much longer, picosecond time scale. Two notable observations emerge for *both* types of excitations: first, there is a delay, Δt , in the onset of the ultrafast decrease in magnetic asymmetry between Fe (51.3 eV) and Ni (66.8 eV); second, for photon energies approximately 2 eV below the Ni edge at 63.7 eV, the transient of the asymmetry initially exhibits a pronounced increase.

For a quantitative analysis, we describe the ultrafast dynamics for both samples by a double ($i = 2$ for 51.3 and 66.8 eV) or triple ($i = 3$ for 63.7 eV) exponential function convolved by a Gaussian function, $G(t)$, with a full width at half maximum (FWHM) reflecting the cross correlation of the XUV and excitation pulse:

$$A(t) = \left(1 + \sum_{i=1}^{2,3} C_i (1 - e)^{-(t-t_0)/\tau_i} \right) \Theta(t - t_0) * G(t), \quad (1)$$

where Θ is the Heaviside function. For the directly excited FeNi/Al(3nm) sample, we set FWHM = 35 fs and vary the amplitudes, C_i , and de- and remagnetization time constants, $\tau_{i=\text{de, re}}$, of the exponential function as well as the overall onset of the dynamics, t_0 . We only consider time-resolved data up to 4 ps. For the direct excitation, we quantify the delayed onset of demagnetization as $\Delta t = t_{0, \text{Ni}} - t_{0, \text{Fe}} = (21 \pm 4)$ fs. We find faster demagnetization times for Ni $\tau_{\text{de, Ni}} = (184 \pm 7)$ fs compared to Fe $\tau_{\text{de, Fe}} = (248 \pm 14)$ fs, but identical rates for the loss of magnetic asymmetry $A/\tau_{\text{de}} = 0.15$ % fs⁻¹, consistent with a number of previous results [1,26]. In order to extract more information about the laser-excited hot electron pulse, we assume that the intrinsic demagnetization time constants, τ_{de} , are independent of the type of excitation, and keep them fixed for the nonlinear fits. Instead, we vary the FWHM of the Gaussian function, yielding an average value of (170 ± 50) fs. Due to the very short duration of the XUV pulses, we can interpret this value as an estimate of the temporal duration of the hot electron pulse. Additionally, we determine the absolute delay for the onset of the magnetization dynamics upon

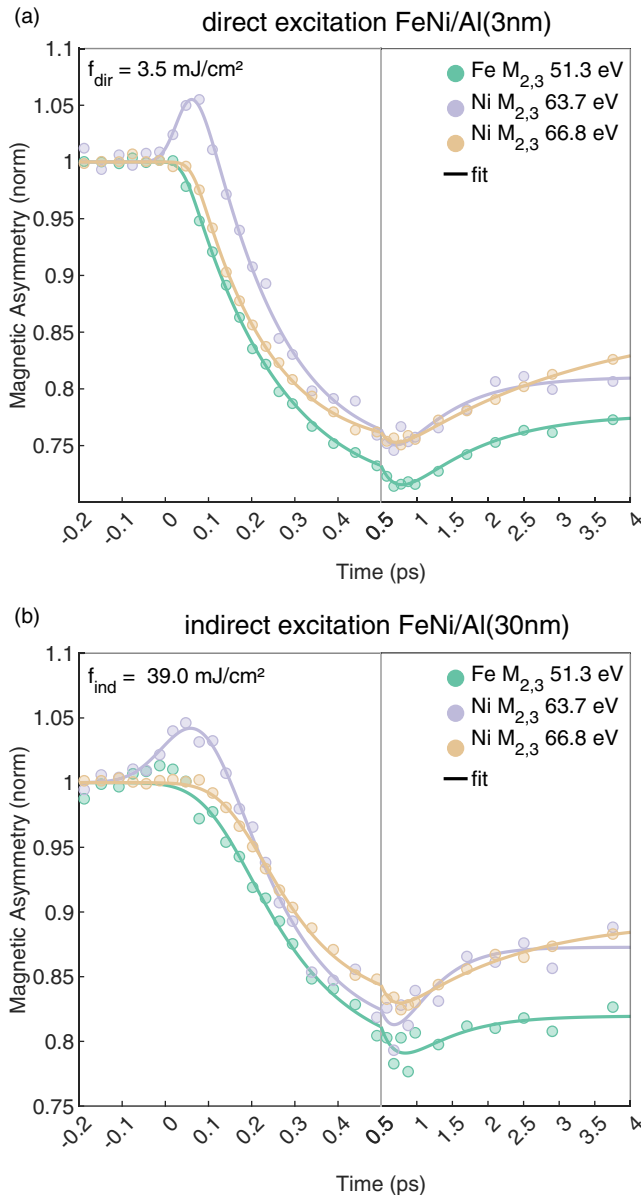


FIG. 3. Ultrafast measured magnetic asymmetry measured at the HHG emission peak energies 51.3, 63.7, and 66.8 eV for (a) direct and (b) indirect excitation for the FeNi alloy. The solid lines represent a best fit to the data points. For either excitation scheme, we observe a delay between the onset of magnetic asymmetry between Fe and Ni as well as an increase of the asymmetry for energies below the Ni resonance. The scaling of the x axis changes at the vertical line at $t = 0.5$ ps.

indirect excitation as approximately $t_{0,Fe} = 70$ fs. We note that the delay between the onset of the magnetization dynamics for Fe and Ni in FeNi/Al(30nm), Δt , increases to 42 fs for the indirect excitation. Finally, the temporal width of the transient increase of A at a photon energy of 63.7 eV increases from approximately FWHM ≈ 70 fs for the direct excitation to approximately 140 fs for indirect excitation. On longer time scales, we observe different demagnetization amplitudes of Fe and Ni, suggesting a distinct temperature dependence of the equilibrium magnetization [38]. The nonlinear least square fits

TABLE I. Parameters describing the ultrafast evolution of the magnetic asymmetry for direct and indirect excitation of the FeNi/Al(5 nm) and FeNi/Al(30 nm) sample. The given error margins correspond to a 1σ -confidence interval. The values marked with an asterisk are kept fixed during the nonlinear least square fitting routines.

	FeNi/Al(5 nm)	FeNi/Al(30 nm)
Fe $M_{2,3}$ 51.3 eV: $t_{0,Fe}$	(0 ± 2) fs	(70 ± 11) fs
Ni $M_{2,3}$ 66.8 eV: $t_{0,Ni}$	(21 ± 2) fs	(112 ± 9) fs
Δt	(21 ± 4) fs	(42 ± 20) fs
Fe $M_{2,3}$ 51.3 eV: τ_{de}	(248 ± 14) fs	248 fs*
Fe $M_{2,3}$ 51.3 eV: A/τ_{de}	$(0.15 \pm 0.02)\%$ fs $^{-1}$	
Ni $M_{2,3}$ 66.8 eV: τ_{de}	(184 ± 7) fs	184 fs*
Ni $M_{2,3}$ 66.8 eV: A/τ_{de}	$(0.15 \pm 0.01)\%$ fs $^{-1}$	
Excitation pulse FWHM	30 fs*	(170 ± 50) fs
A FWHM: 63.7 eV	≈ 70 fs	≈ 140 fs

are shown as solid lines in Figs. 3(a) and 3(b); the parameters of the fits for both types of excitations are summarized in Table I.

IV. DISCUSSION

We would like to begin our discussion by providing a brief evaluation of the current understanding of the magnetic asymmetry measured in T-MOKE experiments. A very recent T-MOKE study revealed that the asymmetry measured at photon energies below the Ni resonance may be influenced by transient spectral reshaping after optical excitation due to changes of the off-axis dielectric tensor [39]. Furthermore, spectral changes of the asymmetry were also found in measurements with photon energies in resonance with the Gd $N_{4,5}$ absorption features and were successfully linked to the ultrafast evolution of magnetization depth profiles [40]. Reshaping of magnetic asymmetry spectra has also been investigated in magnetic circular dichroism studies, both theoretically [41] as well as in a joint experimental-theoretical work [31], and was associated with laser-induced changes of electron occupations. As these effects are most pronounced in the vicinity of the zero crossing of the magnetic asymmetry spectra, we have to acknowledge that the observed increase of A around 63.7 eV may require a more involved analysis to establish its direct and quantitative relationship with the nonequilibrium magnetization. However, we stress that the delayed onset of the Ni demagnetization has been confirmed via well-established L -edge magnetic circular dichroism experiments conducted in transmission geometry [42], affirming its existence with an independent experimental technique.

The main experimental outcome of our paper is that, even when considering an indirect excitation geometry in which significant direct interaction between the light field and the magnetic film can be ruled out, we still detect a delay, Δt , between the onset of the Fe and Ni demagnetization. Furthermore, we also detect an asymmetry increase for photon energies below the Ni $M_{2,3}$ edge. These two fingerprint observables have been previously interpreted as evidence for OISTR—this turns out not to be conclusive in the light of our results. However, one may argue that intersite spin transfer can

occur through ultrafast electron scattering alone, eliminating the need to invoke purely optical spin manipulation for a process to be labeled OISTR.

In our experiment, the nature of the indirect excitation is defined by the lifetimes of hot electrons in Al, which vary between approximately 10 fs at 1.5 eV above E_F and reach up to 60 fs for energy levels less than 0.5 eV above E_F [33]. This implies that electrons within the 30-nm Al layer will experience some scattering events, resulting in a transition from a predominantly ballistic to a diffusive transport behavior. This picture is consistent with our measurements, which reveal an absolute delay $t_{0,Fe} \approx 70$ fs as well as a broadening of the electron excitation pulse to approximately 170 fs. With available Fe minority states in close vicinity to E_F , one could claim that the density-of-state argument holds here as well: now it is electron scattering that populates available Fe minority states, and it is again the availability of Fe states at a suitable energy that sets the direction of a potential intersite spin current. This interpretation is supported by the observation of a significantly longer-lived transient asymmetry increase as well as a larger delay Δt observed in the case of indirect excitation—both caused by the increased temporal width of the electron pulse after its migration through the thick Al layer. This is in line with the expectation that the actual intersite processes between neighboring atoms are ultrafast and hence occur predominantly during the presence of the hot electron excitation pulse.

It is important to note that an interpretation based on incoherent electron scattering presents a different microscopic process compared to coherent intersite dynamics mediated by a spin-selective optical excitation [18]. An interpretation based on such electron scattering dynamics may be consistent with the picture of superdiffusive spin currents [9] as well as with recent theoretical work in which energy and angular momentum are distributed between two sublattices by exchange scattering [23]. Such a scenario would call for an extension of this research to investigate the feasibility of modulating local spin densities through the utilization of *spin-polarized* electrons [43,44], a potentially promising concept for integration into future device applications.

At the same time, we have to concede that our data do not exclude interpretations that do not rely on intersite spin transfer at all, driven neither optically (OISTR) nor electronically, but explain the distinctly different demagnetization

dynamics of Fe and Ni based on different atomic properties of relevance, as for example site-specific spin-orbit coupling [24] or magnon scattering strengths [25,26]. Such site-specific spin-orbit coupling together with ultrafast spin redistribution induced by nearest neighbor electron hopping may also provide an alternative explanation for the observed faster demagnetization times of Pt vs Co in CoPt alloys as well as of Co in CoPt vs single element Co films, previously observed in ultrafast magnetic circular dichroism experiments and attributed to the OISTR effect [19]. The magnon model presents yet another explanation of the delay Δt between the Fe and Ni demagnetization and is based on a preferential magnon generation on Fe sites followed by magnon propagation to neighboring Ni sites [25] and was recently tested in a T-MOKE study with a systematic variation of the stoichiometries x in $Fe_{1-x}Ni_x$ alloys [26].

Finally, we would like to emphasize that our experiments do not, of course, rule out the possibility of coherent light-wave magnetization dynamics. Rather, they demonstrate that the observables previously associated with coherent optical control of the spin system [20,21] fall short of providing unambiguous evidence. Again, more experimental and theoretical work will be essential to help distinguishing the various different proposed microscopic processes and in particular provide reliable evidence for direct and coherent manipulation of magnetization via light.

In conclusion, we have performed a systematic comparison of direct vs indirect excitation of a FeNi alloy via XUV T-MOKE spectroscopy. For both excitation geometries, we find a delayed onset of the loss of magnetic asymmetry of Ni with respect to Fe as well as an increase of the magnetic asymmetry for photon energies below the Ni $M_{2,3}$ edge, signatures which in recent literature have been interpreted as evidence of OISTR, a form of spin manipulation directly driven by light. Our research suggests that secondary processes that emerge after excitation of the electronic system suffice to explain the experimental observations.

ACKNOWLEDGMENTS

We acknowledge financial support by Deutsche Forschungsgemeinschaft Grant No. 328545488 (TRR 227 Project No. A02).

-
- [1] B. Koopmans, G. Malinowski, F. D. Longa, D. Steiauf, M. Fähnle, T. Roth, M. Cinchetti, and M. Aeschlimann, Explaining the paradoxical diversity of ultrafast laser-induced demagnetization, *Nat. Mater.* **9**, 259 (2010).
 - [2] B. Y. Mueller and B. Rethfeld, Thermodynamic μT model of ultrafast magnetization dynamics, *Phys. Rev. B* **90**, 144420 (2014).
 - [3] M. Stiehl, M. Weber, C. Seibel, J. Hofer, S. T. Weber, D. M. Nenno, H. C. Schneider, B. Rethfeld, B. Stadtmüller, and M. Aeschlimann, Role of primary and secondary processes in the ultrafast spin dynamics of nickel, *Appl. Phys. Lett.* **120**, 062410 (2022).
 - [4] A. B. Schmidt, M. Pickel, M. Donath, P. Buczek, A. Ernst, V. P. Zhukov, P. M. Echenique, L. M. Sandratskii, E. V. Chulkov, and M. Weinelt, Ultrafast magnon generation in an Fe film on Cu(100), *Phys. Rev. Lett.* **105**, 197401 (2010).
 - [5] M. Haag, C. Illg, and M. Fähnle, Role of electron-magnon scatterings in ultrafast demagnetization, *Phys. Rev. B* **90**, 014417 (2014).
 - [6] E. Carpena, H. Hedayat, F. Boschini, and C. Dallera, Ultrafast demagnetization of metals: Collapsed exchange versus collective excitations, *Phys. Rev. B* **91**, 174414 (2015).
 - [7] E. Turgut, D. Zusin, D. Legut, K. Carva, R. Knut, J. M. Shaw, C. Chen, Z. Tao, H. T. Nembach, T. J. Silva, S. Mathias,

- M. Aeschlimann, P. M. Oppeneer, H. C. Kapteyn, M. M. Murnane, and P. Grychtol, Stoner versus Heisenberg: Ultrafast exchange reduction and magnon generation during laser-induced demagnetization, *Phys. Rev. B* **94**, 220408(R) (2016).
- [8] S. Eich, M. Plötzing, M. Rollinger, S. Emmerich, R. Adam, C. Chen, H. C. Kapteyn, M. M. Murnane, L. Plucinski, D. Steil, B. Stadtmüller, M. Cinchetti, M. Aeschlimann, C. M. Schneider, and S. Mathias, Band structure evolution during the ultrafast ferromagnetic-paramagnetic phase transition in cobalt, *Sci. Adv.* **3**, e1602094 (2017).
- [9] M. Battiato, K. Carva, and P. M. Oppeneer, Superdiffusive spin transport as a mechanism of ultrafast demagnetization, *Phys. Rev. Lett.* **105**, 027203 (2010).
- [10] B. Vodungbo, B. Tudu, J. Perron, R. Delaunay, L. Müller, M. H. Berntsen, G. Grübel, G. Malinowski, C. Weier, J. Gautier, G. Lambert, P. Zeitoun, C. Gutt, E. Jal, A. H. Reid, P. W. Granitzka, N. Jaouen, G. L. Dakovski, S. Moeller, M. P. Miniti *et al.*, Indirect excitation of ultrafast demagnetization, *Sci. Rep.* **6**, 18970 (2016).
- [11] N. Bergéard, M. Hehn, S. Mangin, G. Lengaigne, F. Montaigne, M. L. M. Laliou, B. Koopmans, and G. Malinowski, Hot-electron-induced ultrafast demagnetization in Co/Pt multilayers, *Phys. Rev. Lett.* **117**, 147203 (2016).
- [12] Y. Xu, M. Deb, G. Malinowski, M. Hehn, W. Zhao, and S. Mangin, Ultrafast magnetization manipulation using single femtosecond light and hot-electron pulses, *Adv. Mater.* **29**, 1703474 (2017).
- [13] S. Iihama, Y. Xu, M. Deb, G. Malinowski, M. Hehn, J. Gorchon, E. E. Fullerton, and S. Mangin, Single-shot multi-level all-optical magnetization switching mediated by spin transport, *Adv. Mater.* **30**, 1804004 (2018).
- [14] Q. Remy, J. Igarashi, S. Iihama, G. Malinowski, M. Hehn, J. Gorchon, J. Hohlfeld, S. Fukami, H. Ohno, and S. Mangin, Energy efficient control of ultrafast spin current to induce single femtosecond pulse switching of a ferromagnet, *Adv. Sci.* **7**, 2001996 (2020).
- [15] Q. Remy, J. Hohlfeld, M. Vergès, Y. L. Guen, J. Gorchon, G. Malinowski, S. Mangin, and M. Hehn, Accelerating ultrafast magnetization reversal by non-local spin transfer, *Nat. Commun.* **14**, 445 (2023).
- [16] J. K. Dewhurst, P. Elliott, S. Shallcross, E. K. U. Gross, and S. Sharma, Laser-induced intersite spin transfer, *Nano Lett.* **18**, 1842 (2018).
- [17] J. Chen, U. Bovensiepen, A. Eschenlohr, T. Müller, P. Elliott, E. K. U. Gross, J. K. Dewhurst, and S. Sharma, Competing spin transfer and dissipation at Co/Cu(001) interfaces on femtosecond timescales, *Phys. Rev. Lett.* **122**, 067202 (2019).
- [18] F. Siegrist, J. A. Gessner, M. Ossiander, C. Denker, Y.-P. Chang, M. C. Schröder, A. Guggenmos, Y. Cui, J. Walowski, U. Martens, J. K. Dewhurst, U. Kleineberg, M. Münzenberg, S. Sharma, and M. Schultze, Light-wave dynamic control of magnetism, *Nature (London)* **571**, 240 (2019).
- [19] F. Willems, S. Sharma, C. v. Korff Schmising, J. K. Dewhurst, L. Salemi, D. Schick, P. Hessian, C. Strüber, W. D. Engel, and S. Eisebitt, Magneto-Optical Functions at the $3p$ Resonances of Fe, Co, and Ni: Ab initio description and experiment, *Phys. Rev. Lett.* **122**, 217202 (2019).
- [20] M. Hofherr, S. Häuser, J. K. Dewhurst, P. Tengdin, S. Sakshath, H. T. Nembach, S. T. Weber, J. M. Shaw, T. J. Silva, H. C. Kapteyn, M. Cinchetti, B. Rethfeld, M. M. Murnane, D. Steil, B. Stadtmüller, S. Sharma, M. Aeschlimann, and S. Mathias, Ultrafast optically induced spin transfer in ferromagnetic alloys, *Sci. Adv.* **6**, eaay8717 (2020).
- [21] P. Tengdin, C. Gentry, A. Blonsky, D. Zusin, M. Gerrity, L. Hellbrück, M. Hofherr, J. Shaw, Y. Kvashnin, E. K. Delczeg-Czirjak, M. Arora, H. Nembach, T. J. Silva, S. Mathias, M. Aeschlimann, H. C. Kapteyn, D. Thonig, K. Koumpouras, O. Eriksson, and M. M. Murnane, Direct light-induced spin transfer between different elements in a spintronic Heusler material via femtosecond laser excitation, *Sci. Adv.* **6**, eaaz1100 (2020).
- [22] D. Steil, J. Walowski, F. Gerhard, T. Kiessling, D. Ebke, A. Thomas, T. Kubota, M. Oogane, Y. Ando, J. Otto, A. Mann, M. Hofherr, P. Elliott, J. K. Dewhurst, G. Reiss, L. Molenkamp, M. Aeschlimann, M. Cinchetti, M. Münzenberg, S. Sharma *et al.*, Efficiency of ultrafast optically induced spin transfer in Heusler compounds, *Phys. Rev. Res.* **2**, 023199 (2020).
- [23] K. Leckron, A. Baral, and H. C. Schneider, Exchange scattering on ultrafast timescales in a ferromagnetic two-sublattice system, *Appl. Phys. Lett.* **120**, 102407 (2022).
- [24] G. Stegmann, W. Töws, and G. M. Pastor, Ultrafast magnetization and energy flow in the laser-induced dynamics of transition metal compounds, *Phys. Rev. B* **107**, 054410 (2023).
- [25] R. Knut, E. K. Delczeg-Czirjak, S. Jana, J. M. Shaw, H. T. Nembach, Y. Kvashnin, R. Stefaniuk, R. S. Malik, P. Grychtol, D. Zusin, C. Gentry, R. Chimata, M. Pereiro, J. Söderström, E. Turgut, M. Ahlberg, J. Åkerman, H. C. Kapteyn, M. M. Murnane, D. A. Arena *et al.*, Inhomogeneous magnon scattering during ultrafast demagnetization, [arXiv:1810.10994v1](https://arxiv.org/abs/1810.10994v1)
- [26] S. Jana, R. Knut, E. K. Delczeg-Czirjak, R. S. Malik, R. Stefaniuk, J. A. Terschlüsen, R. Chimata, D. Phuyal, M. V. Kamalakar, S. Akansel, D. Primetzhofer, M. Ahlberg, J. Söderström, J. Åkerman, P. Svedlindh, O. Eriksson, and O. Karis, Atom-specific magnon-driven ultrafast spin dynamics in $\text{Fe}_{1-x}\text{Ni}_x$ alloys, *Phys. Rev. B* **107**, L180301 (2023).
- [27] D. Schick, udkm1Dsim: A Python toolbox for simulating 1D ultrafast dynamics in condensed matter, *Comput. Phys. Commun.* **266**, 108031 (2021).
- [28] B. Henke, E. Gullikson, and J. Davis, X-ray interactions: Photoabsorption, scattering, transmission, and reflection at $E = 50\text{--}30,000$ eV, $Z = 1\text{--}92$, *At. Data Nucl. Data Tables* **54**, 181 (1993).
- [29] C. von Korff Schmising, S. Jana, K. Yao, M. Hennecke, P. Scheid, S. Sharma, M. Viret, J.-Y. Chauleau, D. Schick, and S. Eisebitt, Ultrafast behavior of induced and intrinsic magnetic moments in CoFeB/Pt bilayers probed by element-specific measurements in the extreme ultraviolet spectral range, *Phys. Rev. Res.* **5**, 013147 (2023).
- [30] In general, a linear relationship between A and the magnetization is only valid for small magnetic contributions to the total reflectance of the nanostructure.
- [31] K. Yao, F. Willems, C. von Korff Schmising, C. Strüber, P. Hessian, B. Pfau, D. Schick, D. Engel, K. Gerlinger, M. Schneider, and S. Eisebitt, A tabletop setup for ultrafast helicity-dependent and element-specific absorption spectroscopy and scattering in the extreme ultraviolet spectral range, *Rev. Sci. Instrum.* **91**, 093001 (2020).

- [32] V. P. Zhukov, E. V. Chulkov, and P. M. Echenique, *GW+T* theory of excited electron lifetimes in metals, *Phys. Rev. B* **72**, 155109 (2005).
- [33] M. Bauer, A. Marienfeld, and M. Aeschlimann, Hot electron lifetimes in metals probed by time-resolved two-photon photoemission, *Prog. Surf. Sci.* **90**, 319 (2015).
- [34] D. L. Windt, IMD: Software for modeling the optical properties of multilayer films, *Comput. Phys.* **12**, 360 (1998).
- [35] *Handbook of Optical Constants of Solids*, edited by E. D. Palik (Elsevier, Amsterdam, 1985).
- [36] J. A. Tossell, Electronic structures of silicon, aluminum, and magnesium in tetrahedral coordination with oxygen from SCF- $X\alpha$ MO calculations, *J. Am. Chem. Soc.* **97**, 4840 (1975).
- [37] A. R. Khorsand, M. Savoini, A. Kirilyuk, and T. Rasing, Optical excitation of thin magnetic layers in multilayer structures, *Nat. Mater.* **13**, 101 (2014).
- [38] M. Hofherr, S. Moretti, J. Shim, S. Häuser, N. Y. Safonova, M. Stiehl, A. Ali, S. Sakshath, J. W. Kim, D. H. Kim, H. J. Kim, J. I. Hong, H. C. Kapteyn, M. M. Murnane, M. Cinchetti, D. Steil, S. Mathias, B. Stadtmüller, M. Albrecht, D. E. Kim *et al.*, Induced versus intrinsic magnetic moments in ultrafast magnetization dynamics, *Phys. Rev. B* **98**, 174419 (2018).
- [39] H. Probst, C. Möller, M. Schumacher, T. Brede, J. K. Dewhurst, M. Reutzler, D. Steil, S. Sharma, G. S. M. Jansen, and S. Mathias, Unraveling femtosecond spin and charge dynamics with extreme ultraviolet transverse Moke spectroscopy, *Phys. Rev. Res.* **6**, 013107 (2024).
- [40] M. Hennecke, D. Schick, T. Sidiropoulos, F. Willems, A. Heilmann, M. Bock, L. Ehrentraut, D. Engel, P. Hessian, B. Pfau, M. Schmidbauer, A. Furchner, M. Schnuerer, C. von Korff Schmising, and S. Eisebitt, Ultrafast element- and depth-resolved magnetization dynamics probed by transverse magneto-optical Kerr effect spectroscopy in the soft x-ray range, *Phys. Rev. Res.* **4**, L022062 (2022).
- [41] K. Carva, D. Legut, and P. M. Oppeneer, Influence of laser-excited electron distributions on the x-ray magnetic circular dichroism spectra: Implications for femtosecond demagnetization in ni, *Europhys. Lett.* **86**, 57002 (2009).
- [42] S. Jana, R. Knut, S. Muralidhar, R. S. Malik, R. Stefanuik, J. Åkerman, O. Karis, C. Schüßler-Langeheine, and N. Pontius, Experimental confirmation of the delayed Ni demagnetization in FeNi alloy, *Appl. Phys. Lett.* **120**, 102404 (2022).
- [43] G.-M. Choi, B.-C. Min, K.-J. Lee, and D. G. Cahill, Spin current generated by thermally driven ultrafast demagnetization, *Nat. Commun.* **5**, 4334 (2014).
- [44] J. Igarashi, W. Zhang, Q. Remy, E. Díaz, J.-X. Lin, J. Hohlfeld, M. Hehn, S. Mangin, J. Gorchon, and G. Malinowski, Optically induced ultrafast magnetization switching in ferromagnetic spin valves, *Nat. Mater.* **22**, 725 (2023).